

# Infrared Spectroscopic Studies of the Reactions of Alcohols over Group IVB Metal Oxide Catalysts

## Part 3.—Ethanol over $\text{TiO}_2$ , $\text{ZrO}_2$ and $\text{HfO}_2$ , and General Conclusions from Parts 1 to 3†

Gamal A. M. Hussein‡ and Norman Sheppard\*

School of Chemical Sciences, University of East Anglia, Norwich NR4 7TJ, UK

Mohamed I. Zaki and Radamis B. Fahim

Chemistry Department, Faculty of Science, Minia University, El Minia 61519, Egypt

The dehydrogenation and dehydration reactions of ethanol over  $\text{TiO}_2$ ,  $\text{ZrO}_2$  or  $\text{HfO}_2$  catalysts has been monitored in the gas phase and on the surfaces by infrared spectroscopy. The reaction pathways closely parallel those of methanol reported in the previous paper (Part 2) with the addition of the direct dehydration reaction  $\text{C}_2\text{H}_5\text{OH} \rightarrow \text{C}_2\text{H}_4 + \text{H}_2\text{O}$  and the production of benzene as a minor product. The infrared spectroscopic analysis of the decomposition of diethyl ether as initial reagent over the  $\text{TiO}_2(500)$  catalyst confirms that the ethane product is derived from the ether precursor. As with methane from methanol, it is probably produced by reduction of the ether to the alkane plus water by hydrogen derived from the parallel dehydrogenation reaction.

A summary is given of probable mechanisms for the catalysed reactions of the three alcohols, methanol, ethanol and propan-2-ol based on the gas-phase products and surface species identified by infrared spectroscopy. The general importance of alkoxide surface intermediates is emphasised. Alkoxides of a given formula occur on different spectroscopically distinguishable sites with different reactivities.

In this third paper of the series, we report results for the catalytic decomposition of ethanol over the Group IVB metal-oxide catalysts,  $\text{TiO}_2$ ,  $\text{ZrO}_2$  and  $\text{HfO}_2$  using infrared spectroscopy. The earlier papers, Parts 1 and 2 (the latter preceding this paper) were concerned with the reactions of propan-2-ol<sup>1</sup> and methanol,<sup>2</sup> respectively, over the same catalysts. The results obtained for ethanol are more similar to those obtained with methanol than with propan-2-ol, but in the present case we have also directly studied the decomposition of the intermediate dehydration product diethyl ether over a hydroxylated  $\text{TiO}_2$  (anatase) catalyst.

A number of previous infrared studies have explored the adsorption of ethanol on, and its reaction over, the oxide catalysts  $\text{TiO}_2(\text{anatase})$ ,<sup>3,4</sup>  $\text{TiO}_2(\text{rutile})$ ,<sup>5,6</sup>  $\text{V/TiO}_2$ ,<sup>7</sup>  $\text{ZrO}_2$ ,<sup>8</sup>  $\text{Al}_2\text{O}_3$ ,<sup>9–12</sup>  $\text{Cr}_2\text{O}_3$ ,<sup>13</sup> and  $\text{MgO}$ .<sup>14</sup> In addition to our recent work on propan-2-ol over the present catalysts,<sup>1</sup> a number of other relevant studies had been made with that alcohol over  $\text{TiO}_2$ <sup>15</sup> and  $\text{CeO}_2$ .<sup>16,17</sup> An infrared study has also been made of diethyl ether adsorbed on  $\text{Al}_2\text{O}_3$ .<sup>18</sup>

### Experimental

The characterization of the catalysts, and the spectroscopic procedures used, have been fully described previously in Parts 1 and 2.<sup>1,2</sup> The  $\text{TiO}_2(300)$  and  $\text{TiO}_2(500)$  catalysts (where the figure in brackets denotes the calcination temperature used for 5 h) have an anatase crystal structure and high specific areas (69.4 and 77.3  $\text{m}^2 \text{g}^{-1}$ , respectively). The strongly dehydroxylated  $\text{TiO}_2(800)$  sample with the rutile structure has a specific area of 14.3  $\text{m}^2 \text{g}^{-1}$ . The  $\text{ZrO}_2(500)$  and  $\text{HfO}_2(500)$  catalysts had specific areas of 2.1 and 12.5  $\text{m}^2 \text{g}^{-1}$ , respectively.

The spectra of the gas phase and of the adsorbed species were recorded following each reaction period of 10 min at a specified temperature *after* the cell had been cooled down to room temperature.

### Reagents, Reference Compounds and Gases

Ethanol and all other chemicals (acetaldehyde, diethyl ether, acetic acid and benzene) were spectroscopic-grade BDH products submitted, prior to an experiment, to degassing by freeze–pump–thaw cycles performed under vacuum. The gases  $\text{O}_2$ ,  $\text{CH}_4$ ,  $\text{CO}_2$  and  $\text{CO}$  were supplied by British Oxygen in high purity (99.99%).

### Results and Discussion

#### Gas-phase Spectra

##### Ethanol over $\text{TiO}_2(300)$

Fig. 1(a)–(c) show that ethanol dominated the gas phase over the anatase  $\text{TiO}_2(300)$  up to 250 °C. After reaction at that temperature, small traces of diethyl ether (band at 1150

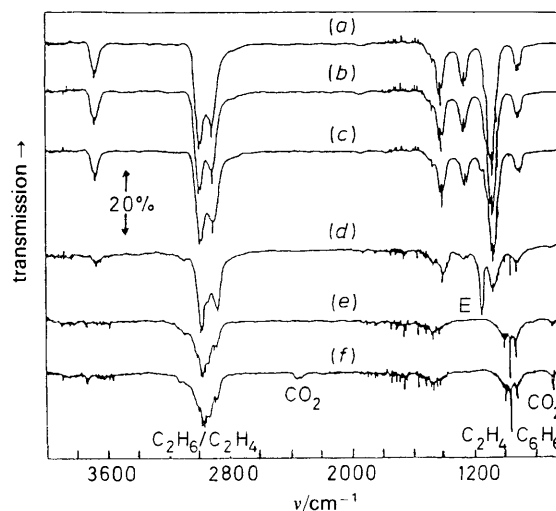


Fig. 1 Room-temperature IR spectra of the gaseous products from the reaction of an equilibrium 10 Torr ethanol over the  $\text{TiO}_2(300)$  catalyst, each taken after allowing the alcohol to interact with the catalyst in a closed cell for consecutive 10 min intervals at: (a) room temperature, (b) 200 °C, (c) 250 °C, (d) 300 °C, (e) 350 °C and (f) 400 °C. E is the diethyl ether

† Part 2: G. A. M. Hussein, N. Sheppard, M. I. Zaki and R. B. Fahim, *J. Chem. Soc., Faraday Trans.*, 1991, 87, 2655.

‡ On leave from Minia University.

$\text{cm}^{-1}$ ) and ethene ( $950 \text{ cm}^{-1}$ ) first occurred. After further reaction at  $300^\circ\text{C}$  [Fig. 1(d)], the first-stage dehydration product, diethyl ether, gave the strongest absorption band below  $1500 \text{ cm}^{-1}$  and ethene (the final dehydration product) had increased in amount; the amount of ethanol present ( $3685 \text{ cm}^{-1}$ ) had decreased by a factor of about three. After reaction at  $350^\circ\text{C}$  [Fig. 1(e)] the spectrum showed that the gas-phase composition had suffered a further radical change; no traces of ethanol or diethyl ether remained, strong absorption bands occurred from ethene and ethane (characterised by its overall gas-phase profile from  $3000$  to  $2800 \text{ cm}^{-1}$ ), and very weak ones appeared from  $\text{CO}_2$  ( $667 \text{ cm}^{-1}$ ) and, unexpectedly, benzene ( $673 \text{ cm}^{-1}$ ). After reaction at  $400^\circ\text{C}$  [Fig. 1(f)], the only further changes were some intensity increases from the absorptions from  $\text{CO}_2$  and benzene, although these still remained relatively very weak. The estimated final composition of the gas phase after reaction at  $400^\circ\text{C}$ , starting from an equilibrium pressure of 10 Torr of the alcohol, was ethane (4), ethene (6),  $\text{CO}_2$  (2), plus small amounts of CO and benzene (1 Torr =  $133.3 \text{ N m}^{-2}$ ).

Results from  $\text{TiO}_2(500)$  were closely similar to those from  $\text{TiO}_2(300)$  and will not be separately discussed.

#### Ethanol over $\text{TiO}_2(800)$

The spectra from the rutile  $\text{TiO}_2(800)$  catalyst were notably different, and are shown in Fig. 2. The most significant differences in relation to the results from  $\text{TiO}_2(300)$  are: (a) ethanol decomposition commenced again at  $250^\circ\text{C}$ , but this time with the production of the dehydrogenation product, acetaldehyde ( $1740 \text{ cm}^{-1}$ ) in the gas phase; this product grew in amount until after  $350^\circ\text{C}$  and remained strong after  $400^\circ\text{C}$ ; (b) ethene production increased from a trace at  $300^\circ\text{C}$  to form a major product after  $400^\circ\text{C}$ ; (c) limited amounts of diethyl ether could be detected after 350 and  $400^\circ\text{C}$ ; (d) complete decomposition of ethanol did not occur until after  $400^\circ\text{C}$ ; (e) after  $400^\circ\text{C}$  substantial absorptions from ethane again occurred, although less than over  $\text{TiO}_2(300)$ , together with again a very weak one from benzene.

The estimated final composition after  $400^\circ\text{C}$  was, in Torr, ethane (2.5), ethene (6), acetaldehyde (2),  $\text{CO}_2$  (1), and again small amounts of CO and benzene.

#### Comparison of the Results over $\text{TiO}_2(300)$ and $\text{TiO}_2(800)$

The principal differences between the results on the hydroxylated  $\text{TiO}_2(300)$  and the dehydroxylated  $\text{TiO}_2(800)$  are the greater importance of the dehydrogenation reaction on  $\text{TiO}_2(800)$  allied with a smaller production of the ether inter-

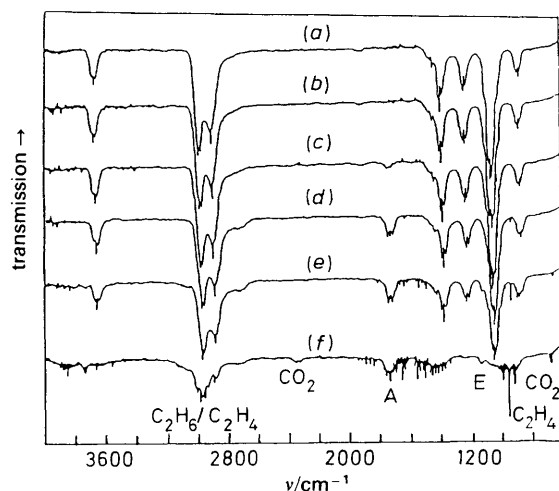


Fig. 2 As for Fig. 1 but for ethanol over the  $\text{TiO}_2(800)$  catalyst. A is acetaldehyde; E are diethyl ether

mediate, and a slower rate of overall ethanol decomposition. Similar differences in the main products between the reactions over these two catalysts occurred also for propan-2-ol<sup>1</sup> and methanol.<sup>2</sup> However, as with the methanol case, notable differences from the propan-2-ol case are the observation once again of the ether intermediate product, and the alkane (ethane) as a final product. The small amounts of benzene as final products at  $400^\circ\text{C}$  finds no counterpart amongst the results from the other two alcohols.

#### Diethyl Ether over $\text{TiO}_2(500)$

As two unexpected features of the ethanol results were the substantial production of the ether over  $\text{TiO}_2(300)$ , limited production over  $\text{TiO}_2(800)$ , and the formation of considerable amounts of ethane as a final product, it was decided to investigate the reactions of diethyl ether itself over  $\text{TiO}_2(500)$ . The gas-phase spectra as a function of the usual temperature regimes are shown in Fig. 3 derived from a starting pressure of ca. 4 Torr of the ether. They show that the ether has begun to dehydrate further to ethene after heating at  $250^\circ\text{C}$ . It had nearly all decomposed after  $300^\circ\text{C}$  but, as from ethanol after  $350^\circ\text{C}$ , strong bands appeared from both ethene and ethane, and a very small amount of benzene could be detected. Further heating at  $400^\circ\text{C}$  led to the production of small amounts of  $\text{CO}_2$  and methane ( $3018$  and  $1307 \text{ cm}^{-1}$ ). The estimated final gas-phase composition after  $400^\circ\text{C}$ , in Torr, was ethane (2.5), ethene (5) and  $\text{CO}_2$  (1.5), plus traces of  $\text{CH}_4$ , CO and benzene. Fig. 4 shows the gas-phase spectrum after heating at  $400^\circ\text{C}$  expanded in the range  $800$  to  $600 \text{ cm}^{-1}$  to show more clearly the  $\text{CO}_2$  and benzene absorptions, in comparison with those from the pure gases.

It is clear from these results that the ethane formation can indeed be correlated with the decomposition of the ether intermediate, as was found to be the case for methanol.<sup>2</sup>

#### Ethanol over $\text{ZrO}_2$ and $\text{HfO}_2$

The infrared gas-phase spectra taken over the variously calcined  $\text{ZrO}_2$  and  $\text{HfO}_2$  catalysts were virtually independent of the catalyst calcination temperature. This is not surprising as all these samples have highly dehydroxylated surfaces. The spectra of the products obtained were also closely similar for the two oxides.

We shall briefly summarise the salient results obtained over the low-surface-area samples of  $\text{ZrO}_2(500)$  and  $\text{HfO}_2(500)$ . In each case, only small amounts of ethanol had decomposed even after the 10 min heating at  $350^\circ\text{C}$ . Acetaldehyde was produced in small amounts after  $250^\circ\text{C}$ , and increasingly until after  $400^\circ\text{C}$ . Ethene commenced to appear

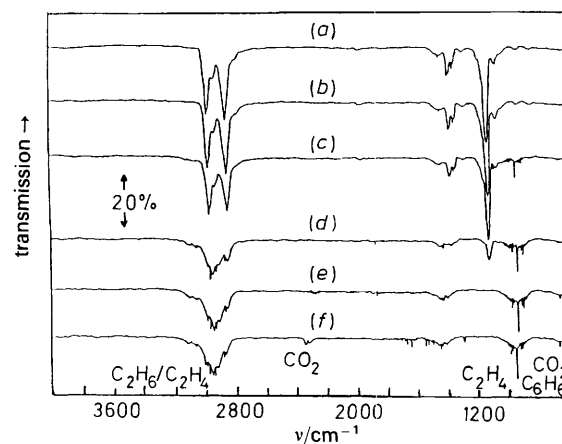
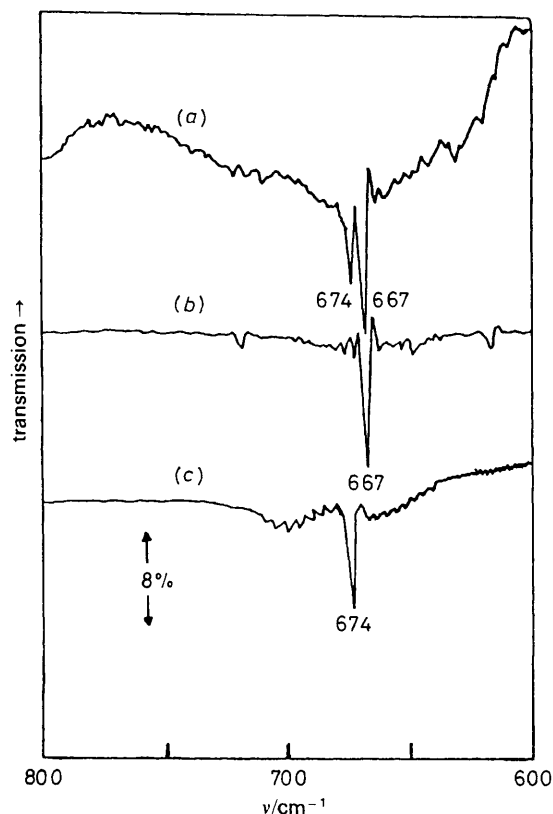


Fig. 3 As for Fig. 1 but for ca. 5 Torr diethyl ether over the  $\text{TiO}_2(500)$  catalyst



**Fig. 4** (a) An expanded portion (800–600  $\text{cm}^{-1}$ ) of the room-temperature IR spectrum [from Fig. 1(f)] of the gas-phase products from ethanol over  $\text{TiO}_2(300)$  after the final heating at 400 °C; reference spectra, at the same resolution, of (b)  $\text{CO}_2$  and (c) benzene

after 300 °C and also increased until 400 °C, at which temperature it was clearly a major product, with acetaldehyde as a minor product, and  $\text{CO}_2$  and methane present in trace quantities. The significant difference from the  $\text{TiO}_2$  results is that no ethane was detected, and nor could the ether be observed as an intermediate product. Other than these differences, the results on  $\text{ZrO}_2$  and  $\text{HfO}_2$  were very similar to those on  $\text{TiO}_2(800)$ , all being catalysts with highly dehydroxylated surfaces.

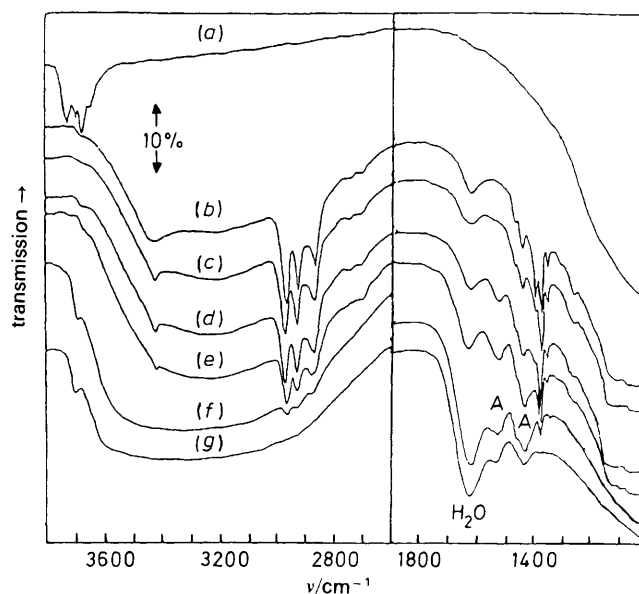
### Spectra from Adsorbed Species

The spectra from adsorbed species, which paralleled the gas-phase results obtained after the different temperature stages, were obtained free of gas-phase contributions by ratioing with the transmission spectrum of the gas phase alone. In a few significant cases, the spectra of the catalysts themselves were also ratioed out. All spectra were measured at room temperature after the relevant heating regimes.

#### Ethanol and Products Adsorbed on $\text{TiO}_2(300)$

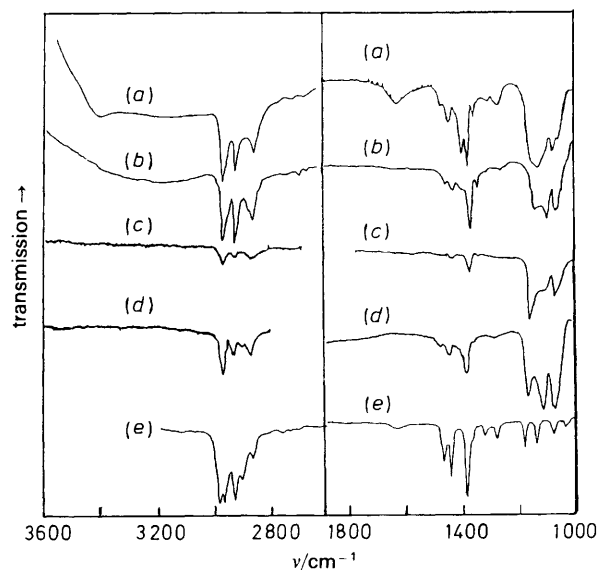
Once again virtually identical results were obtained with the two hydroxylated anatase catalysts  $\text{TiO}_2(300)$  and  $\text{TiO}_2(500)$  and so only those from the former catalyst will be considered. The set of spectra from adsorbed species plus  $\text{TiO}_2(300)$  are shown in Fig. 5. The spectrum, obtained at room temperature after pumping, with additionally the catalyst background ratioed out, is shown in Fig. 6(a). In order to show significant features more clearly, the spectra in Fig. 6 are expanded and only the regions 3600 to 2400  $\text{cm}^{-1}$  and 1900 to 1000  $\text{cm}^{-1}$  are plotted.

Fig. 5(a) illustrates the spectrum of the clean catalyst wafer. Three sharp absorptions at 3720, 3665 and 3640  $\text{cm}^{-1}$  arise



**Fig. 5** Room-temperature IR spectra (3800–2600 and 1900–1000  $\text{cm}^{-1}$ ) of the adsorbed species plus oxide background from ethanol over  $\text{TiO}_2(300)$  at the corresponding stages of reaction to those given in Fig. 1 at: (b), room temperature; (c), 200 °C; (d), 250 °C; (e), 300 °C; (f), 350 °C; and (g), 400 °C; (a) is the spectrum of the oxide before introduction of ethanol. All spectra have been ratioed against the spectrum of the gas phase products. A is surface acetate

from  $\nu_{\text{OH}}$  bond-stretching vibrations of different types of surface OH groups that are free of hydrogen bonding.<sup>1</sup> The adsorption of ethanol at room temperature caused the removal of most of these sharp  $\nu_{\text{OH}}$  bands and the appearance of a broad region of hydrogen-bonded  $\nu_{\text{OH}}$  absorption between 3600 and 3000  $\text{cm}^{-1}$  [Fig. 5(b)]. The sharp  $\nu_{\text{OH}}$   $\text{TiO}_2$  absorptions can be partially restored, with the disappearance of some hydrogen-bonded  $\nu_{\text{OH}}$  absorption, after a brief (5 min) evacuation of the gas phase at room temperature. This shows that a proportion of ethanol molecules were weakly adsorbed by hydrogen bonding to surface OH groups. Titania surface hydroxy groups are known to be weak proton donors.<sup>1</sup>



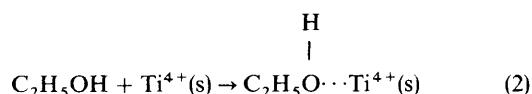
**Fig. 6** Room-temperature IR spectra of adsorbed species after ratioing against the spectrum of the clean oxide disc. Ethanol over: (a),  $\text{TiO}_2(300)$ ; (b),  $\text{TiO}_2(800)$ ; (c),  $\text{ZrO}_2(500)$ ; (d),  $\text{HfO}_2(500)$ ; and (e), diethyl ether over  $\text{TiO}_2(500)$

The absorption at  $1630\text{ cm}^{-1}$ , observed at room temperature [Fig. 5(b) and 6(a)], shows the production of water molecules well before the appearance of the other dehydration product ethene. Analogous to the cases of propan-2-ol<sup>1</sup> and methanol<sup>2</sup> this is considered to be formed by the reaction



where (s) denotes a surface species. All negatively charged surface species are assumed to be coordinatively bonded to surface metal cations. A brief evacuation at  $150^\circ\text{C}$  almost completely eliminated the  $1630\text{ cm}^{-1}$  absorption. At this temperature, the reduction in intensity of the  $1380\text{ cm}^{-1}$  absorption also suggests that this band is caused by the removal of physically adsorbed ethanol, with the implication that the remaining absorptions in the spectrum are from irreversibly adsorbed ethoxide surface species.

The absorptions at room temperature obtained in the  $\nu_{\text{CH}}$  region and below  $1500\text{ cm}^{-1}$  are listed and assigned in Table 1. The  $1270\text{ cm}^{-1}$  absorption which remained with considerable intensity after evacuation at  $150^\circ\text{C}$  is assigned to a  $\delta_{\text{OH}}$  mode of adsorbed alcohol molecules held on to the surface more strongly than by hydrogen bonding. The same assignment to bands in this region has been made in the propan-2-ol case.<sup>12</sup> Such molecules are probably coordinatively bonded to a Lewis-acid site as in (2).



The lack of an analogous absorption on  $\text{TiO}_2(800)$  (see below and Table 1), however, implies that the hydroxylated anatase surface has somewhat different Lewis-acid sites than the dehydroxylated rutile one.

The strong  $\nu_{\text{C-O}}$  absorptions at  $1150$  and  $1100\text{--}1070\text{ cm}^{-1}$  are analogous to a pair at  $1130$  and  $1060\text{ cm}^{-1}$  observed from ethanol on another  $\text{TiO}_2$  sample by Shchekochikhin *et al.*<sup>3</sup> and are there assigned to the presence of two different types of surface ethoxide groups. As discussed in the methanol case,<sup>2</sup> the higher wavenumber band has been assigned to an alkoxide coordinated to a single metal cation, and the lower wavenumber one to an alkoxide bridge-bonded (bidentate) to two adjacent cations.<sup>8,20</sup>

From  $250^\circ\text{C}$  onwards, the ethoxide absorptions gradually weakened and significant new absorptions occurred at  $1540$  and  $1440\text{ cm}^{-1}$  which can clearly be assigned to surface acetate groups.<sup>21</sup> These increased in intensity, with parallel reductions in ethoxide absorptions, until after heating at  $350^\circ\text{C}$ . Heating at  $400^\circ\text{C}$  led them to weaken again while

$\text{CO}_2$  and a small amount of  $\text{CO}$  appeared in the gas phase. The adsorbed water absorption at  $1630\text{ cm}^{-1}$  grew continuously with increasing temperature, in parallel with the production of the dehydration product ethene in the gas phase.

#### Ethanol and Products Adsorbed on $\text{TiO}_2(800)$

The spectrum of the oxide itself in the form of rutile, Fig. 7(a), showed virtually no  $\nu_{\text{OH}}$  absorptions, denoting a highly dehydroxylated surface. Compared with the case on  $\text{TiO}_2(300)$ , the spectra of the adsorbed species at room temperature showed weaker absorption in the  $\nu_{\text{CH}_3}/\nu_{\text{CH}_2}$  and  $\delta_{\text{CH}_3}/\delta_{\text{CH}_2}$  regions, and the virtual absence of the  $1380$  and  $1270\text{ cm}^{-1}$  absorptions attributed above to adsorbed ethanol molecules. Clearly only ethoxide surface species are present, together with a weak and broad hydrogen-bonded  $\nu_{\text{OH}}$  absorption, presumably derived from a residual amount of reaction (1).

After the oxide was heated to  $200^\circ\text{C}$ , the broad  $\nu_{\text{OH}}$  band was converted to a sharper one at  $3420\text{ cm}^{-1}$ , by reaction (3), which has been attributed previously to an OH group on rutile which occurs close to, but not on, the surface.<sup>21,22</sup>



After the oxide was heated at  $250^\circ\text{C}$ , a trace of acetate is first observed ( $1540$  and  $1440\text{ cm}^{-1}$ ), which then grows strongly in parallel with a reduction in intensity of the ethoxide bands and the growth of acetaldehyde in the gas phase, until after heating at  $350^\circ\text{C}$ . These bands weakened again after heating at  $400^\circ\text{C}$ . Absorption from co-adsorbed water increased in intensity from  $250^\circ\text{C}$  in parallel with the production of gas-phase ethene but the total amount was much less than over  $\text{TiO}_2(300)$ .

The ethoxide  $\nu_{\text{C-O}}$  absorptions at room temperature, seen in more detail in Fig. 6b, were more complex than in the  $\text{TiO}_2(300)$  case and once again indicate the presence of more than one ethoxide surface species. The acetate species was the spectroscopically dominant one after heating at  $400^\circ\text{C}$ .

#### Ethanol and Products Adsorbed on $\text{ZrO}_2(500)$ and $\text{HfO}_2(500)$

Typical spectra of adsorbed species, obtained by ratioing-out the absorptions from the catalysts themselves, are shown in Fig. 6(c) for  $\text{ZrO}_2(500)$  and in Fig. 6(d) for  $\text{HfO}_2(500)$ . These are spectra obtained after room-temperature adsorption. The absorption bands and their assignments are listed in Tables 1 and 2. The spectrum at room temperature on  $\text{ZrO}_2$  [Fig. 6(c)] is virtually identical to one recently published elsewhere.<sup>8</sup> As also in the  $\text{HfO}_2$  case, the absorptions in the  $\nu_{\text{C-O}}$  region  $1200\text{--}1000\text{ cm}^{-1}$  show clearly the presence of more than one type of ethoxide surface species, with  $\text{ZrO}_2$  apparently favouring coordination to a single metal cation ( $1160$  strong, with weaker companion bands at  $1120$  and  $1070$

**Table 1** The observed wavenumbers ( $\text{cm}^{-1}$ ) of absorption bands from the surface species produced by reaction of ethanol over  $\text{TiO}_2$ ,  $\text{ZrO}_2$  and  $\text{HfO}_2$  catalysts at room temperature (Fig. 6)

$\text{TiO}_2(300 \text{ and } 500)$	$\text{TiO}_2(800)$	$\text{ZrO}_2(500)$	$\text{HfO}_2(500)$	vibration mode
broad (3600–3000)vs	broad (3600–3100)vw			$\nu_{\text{OH}}$ (H-bonded)
2975s	2975s	2965m	2965w	$\nu_{\text{CH}_3, \text{as}}$
2930s	2930s	2925w	2930w	$\nu_{\text{CH}_2, \text{as}}$
2875s	2875m	2860m	2860w	$\nu_{\text{CH}_3, \text{s}}$
1630m	—	—	—	$\delta_{\text{HOH}}(\text{H}_2\text{O})$
1470w	1450vw	—	—	$\delta_{\text{CH}_2, \text{s}}$
1440m	1440w	1440w	1440w	$\delta_{\text{CH}_3, \text{as}}$
1380s	1380vw	1380mw	1380mw	$\delta_{\text{CH}_3, \text{s}}$ (ethanol)
1360s	1360m	—	—	$\delta_{\text{CH}_3, \text{s}}$ (ethoxide)
1320vw	1320w	—	—	$\text{CH}_2$ wag
1270m	—	—	—	$\delta_{\text{OH}}$ (ethanol)
1150vs	1160s	1160s	1160m	$\nu_{\text{C-O}}/\nu_{\text{C-C}}$ (ethoxides)
1100m	1105s	1120m	1110s	
1070mw	1070s	1070m	1065s	

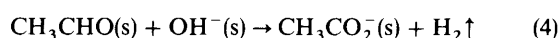
**Table 2** Observed wavenumbers ( $\text{cm}^{-1}$ ) of absorption bands from surface species produced by reaction of ethanol over  $\text{TiO}_2$ ,  $\text{ZrO}_2$  and  $\text{HfO}_2$  catalysts after heating at the reaction temperature of  $400^\circ\text{C}$ 

$\text{TiO}_2(300 \text{ and } 500)$	$\text{TiO}_2(800)$	$\text{ZrO}_2(500)$	$\text{HfO}_2(500)$	acetic acid on $\text{TiO}_2$ at $150^\circ\text{C}$	vibration modes
(3600–3000)vs vbr	ca. 3400m br	—	—		$\nu_{\text{OH}}$ (H-bonded)
2975vw	2970w	2965w	2965w		$\nu_{\text{CH}_3, \text{as}}$
2930vw	2930vw	2930w	2920w		$\nu_{\text{CH}_2, \text{as}}$
—	1700w	2860w	ca. 2860w		$\nu_{\text{CH}_3, \text{s}}$
1630vs	1630m	ca. 1630w, sh	1700w		$\nu_{\text{C=O}}$ of $\text{CH}_3\text{CHO}$
1550s	1530 s	1550vs	ca. 1620w, sh	1560s	$\delta_{\text{HOH}}$ of $\text{H}_2\text{O}$
1440vs	1440vs	1455vs	1550s	1455vs	$\nu_{\text{CO}_2, \text{as}}$
—	—	1430s, sh	1455vs	1430m	$\nu_{\text{CO}_2, \text{s}}$
1380w	1380w	1380vw	1430s, sh	1430m	$\delta_{\text{CH}_3, \text{as}}$
			1380vw	1380w	$\delta_{\text{CH}_3, \text{s}}$

$\text{cm}^{-1}$ ) and  $\text{HfO}_2$  favouring coordination to two adjacent cations (1100 and  $1056$  strong, with a weaker companion at  $1160$   $\text{cm}^{-1}$ ).

In the spectra from both oxides, acetate absorptions appeared at  $250^\circ\text{C}$  and grew in intensity until after heating at  $350^\circ\text{C}$ . Over the same temperature range, acetaldehyde had increased in the gas phase, while surface ethoxide diminished. It was particularly clear with  $\text{ZrO}_2$  that, in the presence of ethanol, the  $1160$   $\text{cm}^{-1}$  band of the ethoxide diminished first while acetaldehyde appeared in the gas phase. The ca.  $1060$   $\text{cm}^{-1}$  absorption decreased more slowly at a time when ethene was appearing in the gas phase. This suggests that the single-coordinated ethoxide may react to form acetaldehyde (which partially further oxidises to acetate) while the doubly coordinated ethoxide may react to form ethene. Over  $\text{TiO}_2(800)$ , it is not so easy to follow the temperature dependence of the broader  $1160$   $\text{cm}^{-1}$  band (Fig. 7), although the sharper  $\nu_{\text{C-O}}$  absorptions at  $1105$  and  $1070$   $\text{cm}^{-1}$  persist up to higher temperatures. This correlation cannot be carried directly through to the hydroxylated  $\text{TiO}_2(300)$  case, as the  $1160$   $\text{cm}^{-1}$  absorptions are strong in that case also but no acetaldehyde appears in the gas phase. However, acetate species do occur on the surface starting at  $250^\circ\text{C}$ , and it may be that on the anatase surface the aldehyde is immediately surface-oxidised to the carboxylate according to the equa-

tion:



At  $400^\circ\text{C}$  on  $\text{HfO}_2$ , a weak band at  $1700$   $\text{cm}^{-1}$  probably denotes some adsorption of acetaldehyde on the surface, and residual amounts of both types of ethoxide remained. As was clear from the gas-phase spectra,  $\text{HfO}_2$  is a less active catalyst than  $\text{ZrO}_2$ .

#### Diethyl Ether and adsorbed products from $\text{TiO}_2(500)$

The spectra of the adsorbed species plus oxide are shown in Fig. 8 and expanded versions, ratioed against the oxide background, are shown in Fig. 6(e).

At room temperature, Fig. 8(a), the sharp  $\nu_{\text{OH}}$  bands from the hydroxylated  $\text{TiO}_2(500)$  surface are shifted into a broad hydrogen-bonded  $\nu_{\text{OH}}$  band at ca.  $3200$   $\text{cm}^{-1}$ . This shows that in part the ether is physically adsorbed *via* hydrogen bonding to the surface OH groups. This is confirmed by evacuation when the sharp surface  $\nu_{\text{OH}}$  bands are considerably restored. However, there still remain strongly adsorbed species, Fig. 6(e), giving absorptions in the  $\nu_{\text{CH}}$  region at  $2985$ ,  $2965$ ,  $2930$ ,  $2905$  and  $2870$   $\text{cm}^{-1}$  and, below  $1500$   $\text{cm}^{-1}$ , at  $1470$ ,  $1460$ ,  $1380$ ,  $1280$ ,  $1180$ ,  $1140$  and  $1080$   $\text{cm}^{-1}$ . The different wavenumbers and greater complexity of this spectrum relative to that described earlier from ethoxide surface species

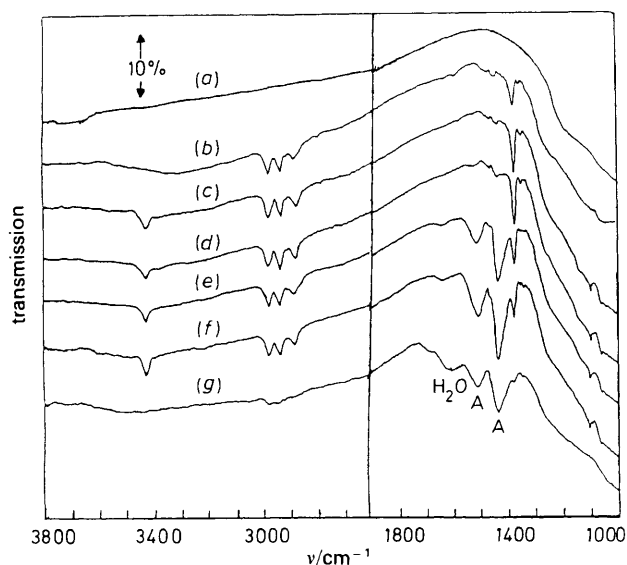


**Fig. 7** As for Fig. 5, but for ethanol over  $\text{TiO}_2(800)$ : (b) room temperature; (c),  $200^\circ\text{C}$ ; (d),  $250^\circ\text{C}$ ; (e),  $300^\circ\text{C}$ ; (f),  $350^\circ\text{C}$ ; (g)  $400^\circ\text{C}$ ; (a) is the spectrum of the oxide before introduction of ethanol. A is surface acetate

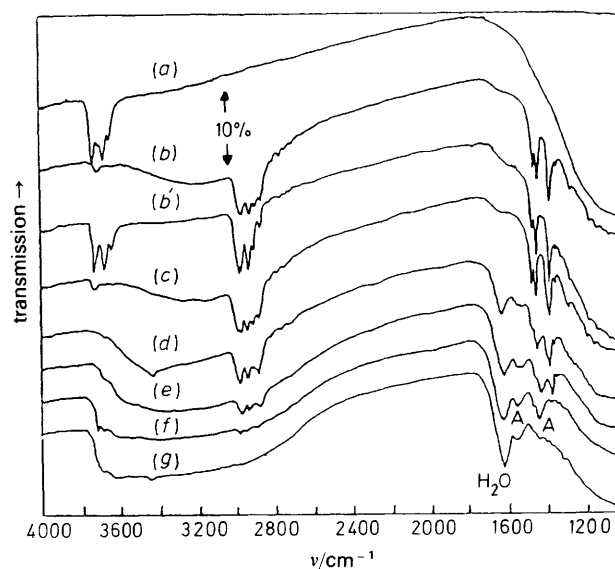


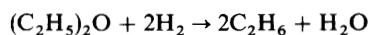
**Fig. 8** As for Fig. 5, but for diethyl ether over  $\text{TiO}_2(500)$ : (b) room temperature; (b'), room temperature after evacuation for 10 min; (c),  $200^\circ\text{C}$ ; (d),  $250^\circ\text{C}$ ; (e),  $300^\circ\text{C}$ ; (f),  $350^\circ\text{C}$ ; and (g),  $400^\circ\text{C}$ ; (a) is the spectrum of the oxide before introduction of the diethyl ether. A is the surface acetate

imply the presence of coordinatively bound diethyl ether. After the oxide was heated at 250 °C and higher temperatures, the spectrum profile in the  $\nu_{\text{CH}}$  region becomes that associated with ethoxide species. The usual acetate bands, plus increased 1630  $\text{cm}^{-1}$  absorption from adsorbed water, grew in strength with further temperature rise, while the ethoxide bands diminished in the usual way. The dehydration product, ethene, appeared increasingly in the gas phase.

### Origins of the Products Ethane and Benzene

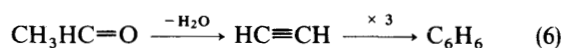
A straightforward explanation of the formation of ethane might seem to be that the  $\text{TiO}_2$  surfaces also catalyse the reaction of the ethene, produced by dehydration, with the hydrogen produced by the dehydrogenation reaction. However, although other oxides, such as  $\text{ZnO}$ ,<sup>23,24</sup> can catalyse the hydrogenation of alkenes, it is difficult to understand, on this hypothesis, why propane is not likewise produced from the reaction of propan-2-ol over the same  $\text{TiO}_2$  catalysts. Furthermore, this explanation cannot be applied to the equally ready formation of methane from methanol over the same catalysts, as reported in Part 2.

However, as in the case of the production of methane from methanol, we have shown (this time starting from the ether itself) that ethane is also generated by the reaction of diethyl ether over the hydroxylated surface of  $\text{TiO}_2(500)$ . It is probable that, as postulated in the methanol case, it is produced by dehydrogenation of the ether according to the overall reaction



In this case, however, it was not possible to obtain an indication that water is the other product from the reaction because of the presence of the parallel direct dehydration of ethanol to ethene. This complication was not present in the methanol case.<sup>2</sup>

The minor product benzene is probably derived from trimerisation of acetylene, which in turn might be catalytically produced by dehydration of acetaldehyde, *i.e.*



Although the first step of this reaction sequence is not thermodynamically favoured at equilibrium, the immediate conversion of acetylene to benzene could cause the reaction to continue.

### General Conclusions for Parts 1–3

#### Experimental Methods

Looking back over the results obtained in these studies of the three alcohols, it is clear that the infrared method has many advantages for following the simultaneous chemical changes in both the gas and solid phases of closed systems such as those investigated here. As far as the gas phase is concerned, infrared spectra are capable of unambiguous identification (and often quantitative evaluation) of virtually all small or medium-sized reactants and products, including unexpected ones. The only exceptions are the symmetrical diatomic molecules such as  $\text{H}_2$  (relevant in the present case)  $\text{O}_2$ ,  $\text{N}_2$ ,  $\text{Cl}_2$  *etc.*, which do not have infrared absorption bands. In the particular cases of these alcohol-reactivity studies, the infrared spectra of the catalyst discs, after computer-subtraction of the gas-phase contributions, have also proved to be remarkably successful at identifying and qualitatively evaluating the amounts of surface species present at any given stage of the gaseous reaction. The measurements have only been qualitative in the sense that we have not had available to us cali-

bration infrared data that would enable us to do quantitative analysis on the adsorbed species. In principle, however, such information should be obtainable, at least for those adsorbed species that can be studied one at a time on catalyst discs of the same size and weight.

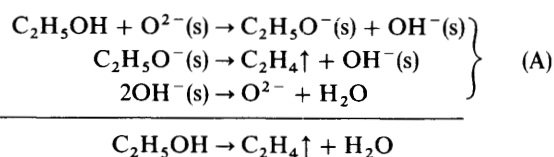
The experimental procedures used in this work involving heating the gas phase for fixed intervals of time at various temperatures followed by quenching the reaction by cooling to room temperature, has been used by two of us before on the propan-2-ol/ $\text{CeO}_2$  system.<sup>16</sup> However the present work has brought out more clearly the power of the method. The return to room temperature after each phase of the reaction is essential if accurate infrared evaluations are to be achieved by spectral subtraction techniques. In particular, the spectra of solids at elevated temperatures can have substantial mixtures of emission and transmission contributions. Not only does this make the spectra difficult to interpret, but highly accurate temperature control is required if a background catalyst spectrum is to be ratioed-out in order to reveal the absorption bands of the adsorbed species. Carrying out such ratioing procedures at room temperature is altogether a more straightforward procedure, as the detector is essentially at the same temperature as the sample.

### Results and Reaction Pathways of the Chemical Reactions

With the help of the separate spectra of the gas phase and catalyst discs, several of the catalytic processes involved seem to be identifiable.

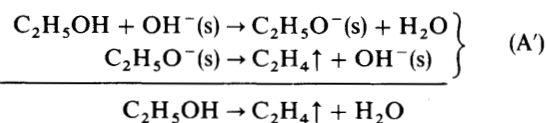
#### Dehydration Reactions

One-molecule dehydration applies to the cases of ethanol and propan-2-ol. Assuming an  $\text{OH}^-$ -free surface, as with  $\text{TiO}_2(800)$ ,  $\text{ZrO}_2(500)$  and  $\text{HfO}_2(500)$ , the mechanism appears to be in outline (taking for simplicity the ethanol example)



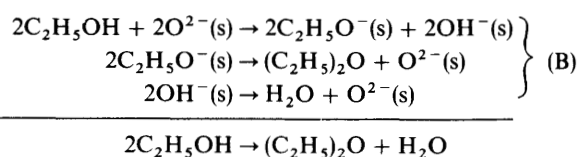
The details for the second  $\beta$ -H elimination step may for geometric reasons involve  $\text{H}^-$  donation to an  $\text{M}^{4+}$  cation ( $\text{M} = \text{Ti}, \text{Zr}, \text{Hf}$ ), followed by its rapid transfer to the O atom during the breaking of the C–O bond.

An alternative dehydration process that probably occurs on an  $\text{OH}^-$ -rich oxide surface, such as those of  $\text{TiO}_2(300)$  or  $\text{TiO}_2(500)$ , is

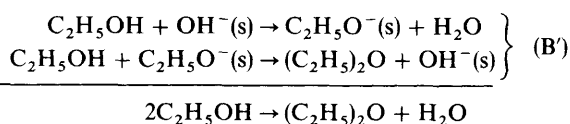


The water production occurs during the first step and may lead to the  $\text{OH}^-$ -rich surfaces having greater selectivity for dehydration. A further contributory factor may be the blocking of the Lewis-acid sites required for dehydrogenation by the surface  $\text{OH}^-$  ions.

The two-molecule dehydration reaction to give ethers is in principle applicable to all three alcohols, but in practice did not occur with propan-2-ol. On an  $\text{OH}^-$ -free surface it can occur as



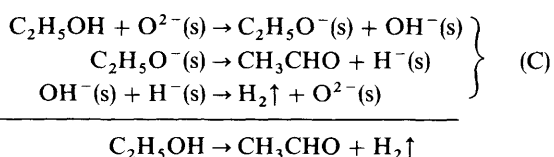
On an OH<sup>-</sup>-rich surface the alternative could be



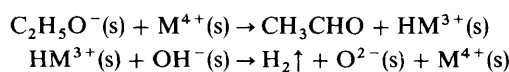
The absence of ether-production from propan-2-ol most probably occurs because of the greater steric factor involved in the reaction together of two adjacent alkoxide ions, or of an alkoxide ion and an alcohol molecule.

#### Dehydrogenation Reactions

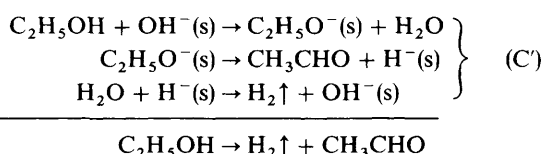
On the OH<sup>-</sup>-free surface the mechanism seems likely to be:



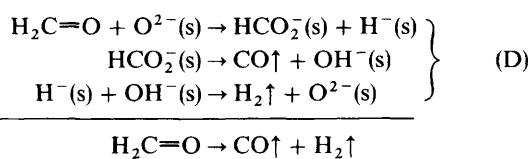
The second  $\alpha$ -H elimination step and its successor in (C) can be formulated in more detail as



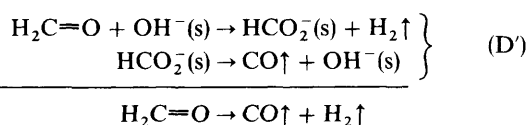
On an OH<sup>-</sup>-rich surface the alternative course for the dehydrogenation reaction could be



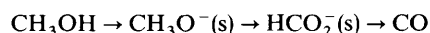
We have found experimental evidence, in the case of methanol, for the strong participation of a second dehydrogenation step at higher temperatures. Based on formaldehyde produced by the first step, this can be formulated as



or as



Formate ions, HCO<sub>2</sub><sup>-</sup>(s), are very much in evidence in the spectra of the catalyst discs, rather more so for the OH<sup>-</sup>-free surfaces. Their proposed activity as an intermediate fits very well with an earlier excellent kinetic demonstration by Tamaru *et al.*<sup>25</sup> that the formate ion is a reaction intermediate in the reaction



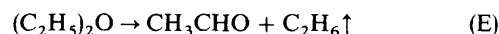
catalysed by ZnO.

Although in the case of ethanol, the corresponding acetate ion is also prominent in the spectra of the surface species, this is strongly retained even after heating to 400 °C on the OH<sup>-</sup>-rich and OH<sup>-</sup>-free surfaces, and only leads to minor amounts of products such as CO<sub>2</sub>, CO and methane. For propan-2-ol, higher temperatures clearly lead to some C—C bond scission, as shown by the presence of spectroscopically identifiable surface acetate ions.

#### Production of Alkanes

We turn next to the postulated mechanisms for the formation of methane and ethane from methanol and ethanol, respectively. We have found good experimental evidence that the ether dehydration product is involved as a reaction intermediate, and the lack of observation of the ether from propan-2-ol provides a rationalisation for the non-observation of an alkane product (propane) in that case.

We have considered two possible mechanisms. The first is essentially an ether disproportionation reaction of the form (E), presumably mediated by surface adsorption.

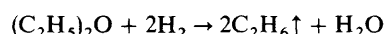
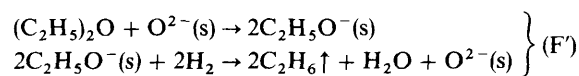
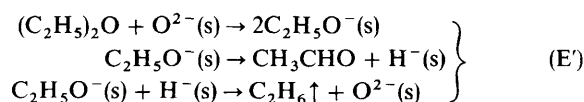


Acetaldehyde is also independently produced by dehydrogenation of ethanol.

The second alternative is a reaction involving hydrogen generated by the parallel dehydrogenation reaction, according to equation (F)



Either or both of these probably proceed *via* ethoxide intermediate species as in (E') or (F').



There is evidence, Fig. 6(e) and 8, that when the reaction is initiated from the diethyl ether itself, the adsorbed ether is retained on the surface to 200 °C but is thereafter converted to ethoxide. The production of ethane occurs above 250 °C.

We have given a reason, based on water production in parallel with methane production in the methanol case,<sup>2</sup> for preferring reaction (F/F') to (E/E').

#### General Comments

The above mechanisms provide suggestions for the production of the major products in terms of surface intermediates, all of which have been identified as present in substantial amounts. No other substantial surface species have been detected except thermally stable acetate ions, and only minor amounts of the additional products, benzene (from ethanol) and methane and CO<sub>2</sub> (from ethanol and propan-2-ol) have been found in the gas phase. It has been postulated that the latter two come from the high-temperature thermal decomposition of acetate ions.<sup>1</sup>

#### Role of Surface Alkoxide Ions

The reaction sequences, (A)–(D), (E') and (F'), all involve surface alkoxide ions in one role or another. There is direct evidence, based on earlier studies by the Lavalley<sup>8</sup> and Tsyganenko<sup>20</sup> research groups, that surface species of this kind do occur in different forms on oxide surfaces, as shown for example by the infrared observation of two  $\nu_{\text{C-O}}$  modes from methoxide. The presence of these different species has been confirmed by the present infrared work. The earlier proposed attributions of the high-wavenumber absorption to monodentate methoxy [*i.e.* interaction with a single M<sup>4+</sup>(s) ion] and the low wavenumber mode to the bidentate species (presumably formed on a more coordinatively unsaturated part of the surface) seem reasonable. We have found some evidence over ZrO<sub>2</sub> that the high-wavenumber band is the

first to weaken on raising the reaction temperature into the temperature range where the dehydrogenation reaction is the first and principal one occurring. The alternative dehydration reactions [(A) and (A')] involve the retention on the surface of oxygen atoms from the alkoxide, and it is at least plausible that this is most likely to occur with the more strongly held bidentate species. There do not seem to be grounds from the spectroscopic data to consider that the situation is as simple as this, but such possibilities do provide an incentive for particularly careful future studies of the relationship between the changes in amount of the different alkoxide species and products being produced, and also of the sites that the spectroscopically distinguishable alkoxides occupy on the oxide surfaces.

In the case of adsorption on metal surfaces, a great deal of specific information about the sites occupied by adsorbed species has been obtained by carrying out spectroscopic work on single-crystal planes of known atomic arrangements.<sup>26,27</sup> Although such work on oxides is likely to be more difficult for a variety of reasons, not least the lack of availability of suitably sized regular crystals, recently a start has been made on the spectroscopic study of adsorption on single crystals of MgO<sup>28</sup> and ZnO.<sup>29</sup> No such work seems yet to have been carried out by infrared spectroscopy, although photon spectroscopies have the advantage that they do not lead to charge build-up on the surface. Vibrational electron energy loss spectroscopy (VEELS) has greater sensitivity but can cause surface-charging effects.

An alternative method of assigning  $\nu_{C-O}$  modes of alkoxide species to adsorption sites on particular surfaces would be to carry out infrared studies on highly crystalline particulate oxides of known and uniform crystal habit. High-temperature flame production of the oxide, such as the preparation of MgO 'smoke', can lead to the thermodynamically most favourable faces being dominant with edge and corner sites in minority.<sup>30,31</sup> Much interesting work remains to be done on the surface-catalysed reactions of these and other types of reagents.

G.A.M.H. thanks the Egyptian Government for maintenance and travel grants. N.S. thanks the SERC for financial assistance with infrared spectroscopic equipment.

## References

- 1 Part 1. G. A. M. Hussein, N. Sheppard, M. I. Zaki and R. B. Fahim, *J. Chem. Soc., Faraday Trans. 1*, 1989, **85**, 1723.

- 2 Part 2. G. A. M. Hussein, N. Sheppard, M. I. Zaki and R. B. Fahim, *J. Chem. Soc., Faraday Trans. 1*, 1991, **87**, 2655.
- 3 Y. M. Shchekochikhin, V. N. Filimonov, N. P. Keier and A. N. Terenin, *Kinet. Catal.*, 1964, **5**, 94 (Russian edn., p. 113).
- 4 I. Carrizosa and G. Munuera, *J. Catal.*, 1977, **49**, 174.
- 5 P. Jackson and G. D. Parfitt, *J. Chem. Soc., Faraday 1*, 1972, **68**, 1443.
- 6 Y. Suda, T. Morimoto and M. Nagao, *Langmuir*, 1987, **3**, 99.
- 7 H. Miyata, Y. Nakagawa, T. Ono and Y. Kubokawa, *J. Chem. Soc., Faraday Trans. 1*, 1983, **79**, 2343.
- 8 M. Bensitel, V. Moravek, J. Lamotte, O. Sauer and J-C. Lavalley, *Spectrochim. Acta, Part A*, 1987, **43**, 1487.
- 9 A. A. Babushkin and A. V. Uvarov, *Dokl. Acad. Sci. USSR*, 1956, **110**, 581.
- 10 R. G. Greenler, *J. Chem. Phys.*, 1962, **37**, 2094.
- 11 R. O. Kagel, *J. Phys. Chem.*, 1967, **71**, 844.
- 12 W. Hertl and A. M. Cuenca, *J. Phys. Chem.*, 1973, **77**, 1120.
- 13 L. M. Roev and A. N. Terenin, *Dokl. Acad. Sci. USSR*, 1959, **124**, 373.
- 14 R. O. Kageland and R. G. Greenler, *J. Chem. Phys.*, 1968, **49**, 1638.
- 15 R. F. Ross, G. Busca, V. Lorenzelli, O. Sauer and J-C. Lavalley, *Langmuir*, 1987, **3**, 52.
- 16 M. I. Zaki and N. Sheppard, *J. Catal.*, 1983, **80**, 114.
- 17 M. I. Zaki, G. A. M. Hussein, H. A. El-Ammawy, S. A. Mansour, J. Polz and H. Knözinger, *J. Mol. Catal.*, 1990, **57**, 367.
- 18 A. V. Kiselev and A. V. Uvarov, *Surf. Sci.*, 1967, **6**, 399.
- 19 C. G. Barraclough, D. C. Bradley, J. Lewis and I. M. Thomas, *J. Chem. Soc.*, 1961, 2601.
- 20 A. A. Tsyganenko and V. N. Filimonov, *J. Mol. Struct.*, 1973, **19**, 579.
- 21 J. Graham, C. H. Rochester and R. Rudham, *J. Chem. Soc., Faraday Trans. 1*, 1981, **77**, 1973.
- 22 J. Graham, C. H. Rochester and R. Rudham, *J. Chem. Soc., Faraday Trans. 1*, 1981, **77**, 2735.
- 23 R. J. Kokes and A. L. Dent, *Adv. Catal.*, 1972, **22**, 1.
- 24 C. S. John, *Catalysis*, Specialist Periodical Report, The Chemical Society, London, 1980, vol. 3, p. 169.
- 25 A. Ueno, T. Onishi and K. Tamaru, *Trans. Faraday Soc.*, 1971, **67**, 3585.
- 26 N. Sheppard and T. T. Nguyen, *Adv. Infrared Raman Spectrosc.*, 1978, **5**, 67.
- 27 N. Sheppard, *Annu. Rev. Phys. Chem.*, 1988, **39**, 589.
- 28 H. Onishi, C. Egawa, T. Aruga and Y. Isawara, *Surf. Sci.*, 1987, **191**, 479.
- 29 J. M. Vohs and M. A. Barteau, *Surf. Sci.*, 1989, **221**, 590.
- 30 S. Collucia, A. J. Tench and R. L. Segall, *J. Chem. Soc., Faraday Trans. 1*, 1979, **75**, 1769.
- 31 C. F. Jones, R. A. Reeve, R. Rigg, R. L. Segall, R. St. C. Smart and P. S. Turner, *J. Chem. Soc., Faraday Trans. 1*, 1984, **80**, 2609.